INDIAN INSTITUTE OF TECHNOLOGY, KANPUR

SURGE 2024

Project Report

"A SIGNAL TO NOISE ESTIMATOR FOR EXOPLANET CHARACTERIZATION USING CUBESATS"

Submitted by

Akshita Agarwal

Application number: 2430176

Department Of Chemistry

IIT Kanpur (U.P.)

Under the guidance of

Professor Prashant Pathak

Department of Space, Planetary & Astronomical Sciences & Enguneering (SPASE)

IIT Kanpur (U.P.)

Abstract

Our project aims to develop a simulation platform for estimating exoplanetary signals in spectroscopic mode based on a given aperture size. The platform will provide insights into characterizing different types of exoplanets and the time required for observations. We will leverage data from the simulator to inform the design and observation constraints for CubeSat missions. The code generates graphs that aid in understanding the exoplanet's atmosphere, which is essential for characterizing exoplanets. Our primary objective was to optimize the existing code to enhance its efficiency and comprehensibility, making it more accessible for future development and collaboration.

Table of Contents

Introduction

Exoplanets have long fascinated humans, and the search for life on these planets has been a major goal. Advancements in technology now allow us to determine the habitability of planets, but we are still far from our goal. CubeSats, such as the Colorado Ultraviolet Transit Experiment (CUTE) mission launched in September 2021, are designed to detect and understand the composition of exoplanets and their atmosphere. This mission provided valuable information about the atmospheres of over 100 hot Jupiters, including the presence of elements such as Fe, Mg, and OH atoms. Each planet has unique features and elements, making their study extremely fascinating. Our work was inspired by the desire to create a Signal to Noise calculator for exoplanet characterization using CubeSats. Our main aim was to develop a simulation platform to estimate exoplanetary signals in spectroscopic mode for a given aperture size, providing insights into characterizing different types of exoplanets and the time required for observations.

Methodology

We utilized the following functions, properties, and phenomena in the code:

Gaussian kernel and sigma: The Gaussian distribution accounts for the thermal motion of atoms, while the Lorentzian distribution represents the natural broadening of spectral lines. The code covers 4σ, where 4σ is approximately equal to 3.397, as 99.99% of the data lies within +-(4σ). This multiplication of σ by 4 ensures that the Gaussian kernel spreads far enough to avoid generating errors.

Lorentzian: L(v)=$\pi[(v - v0) \times 2 + \gamma^2]\gamma$

Voigt Profile: It is a convolution of a Gaussian and a Lorentzian distribution, widely used in spectroscopic analysis to describe the line shape of a spectral line and account for the broadening effect.

V(v)= $\int_{-\infty}^{\infty} \mathrm{G}(\nu')\mathrm{L}(\nu - \nu')\, dv'$

ISM (Interstellar Medium): It includes matter between stars and galaxies, such as gas, dust, cosmic rays, etc. When light passes through the ISM, phenomena such as extinction, reddening, and spectral line absorption or emission can alter the wavelengths

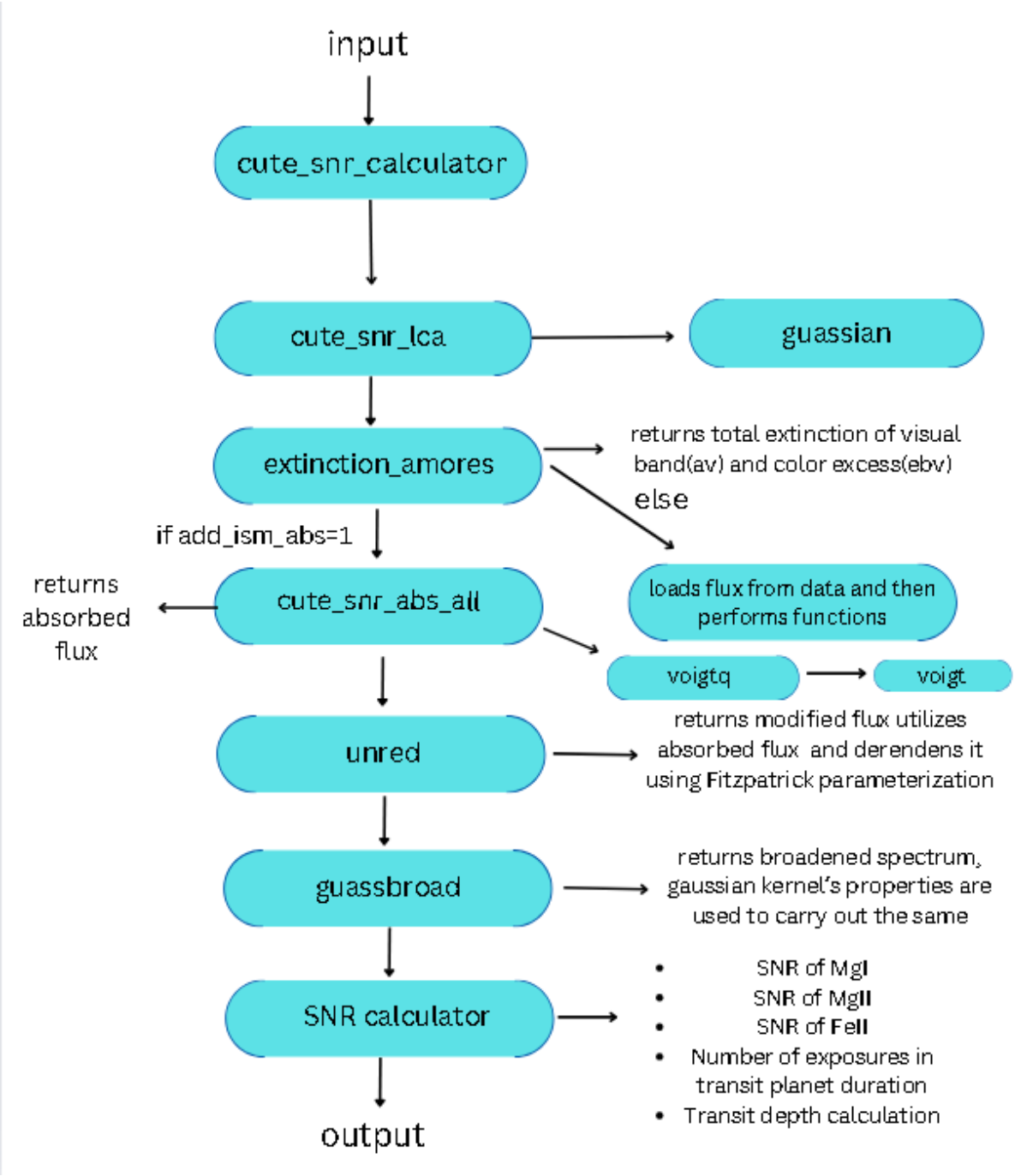

Fig: Flow of code

The following are the input parameters required by the code:

1.Temperature of the star in Kelvin
2. Radius of the star in solar radius
3. Mass of the star
4. Distance to the star as parallax in milliarcseconds
5. Coordinates of the star (Right ascension and declination)- this information is used to calculate the extinction and ISM column densities
6. Stellar activity index ($\log R\ HK$)of the star. This parameter sets the strength of the MgII h&k line core emission

7. Spectral resolution: Spectral resolution of the spectrograph in angstroms
8. CCD readout noise: The CCD readout noise in $electrons\ pixels^{-1}$
9. CCD dark noise: The CCD dark noise in $electrons\ pixels^{-1}s^{-1}$
10. CCD gain: The CCD gain in photoelectrons ADU^{-1}
11. Spectrum width: Expected width in the cross-dispersion direction of the spectrum in pixels
12. Exposure time: Exposure time for each observation in seconds
13. CCD read time: The CCD read time for each observation in seconds

The "Cute_snr_calculator" initially loads the file for the respective planet corresponding to the input temperature and calls the function "cute_snr_lca" for flux calculation.

- The "cute_snr_lca" function first checks if the spectral type, radius of the star, and BV are defined. If not, it sets the values corresponding to the nearest temperatures. Then, it calculates the MgIIh wavelength (2795.5280), MgIIh $\log gf$ (0.100), MgIIh stark(-5.680), MgIIk wavelength (2802.7050), and MgIIkStark damping constant (-5.680). The function then calculates the ratio of the oscillator strengths for the MgII k line to the MgII h line using their respective $\log gf$ values. Mg21 emission is calculated using $\frac{E}{(1+\mathrm{Mgaratio}_{\mathrm{loggf2to1}})}$
where E is E=$(\mathrm{Rmg}\ \times \mathrm{AU})^2$.
Gaussian functions are created for the Mg II k and h lines. It then calls the Gaussian function to obtain the emitted flux of MgI and MgII+ ions and adds the two to obtain Mg ions flux. The parameters for the Gaussian function include the wavelength, the central wavelength (MgII2w and MgII1w), the width (σMg22 and σMg21), and the peak value (0.3989 x Mg22em / σMg22 and 0.3989 * Mg21em / σMg21).

Gaussian: computes Gaussian function centered around w10 by using

$$1 \times e^{-0.5(\frac{wavelength-w10}{\sigma})\text{^}2}$$

- The "extinction_amores" function helps obtain the interstellar extinction in the galaxy based on the model by Amores & Lépine (2004). This extinction represents the dimming of light from stars and other celestial objects due to interstellar dust and gas. The simulator takes every wavelength in the defined range with a difference of 1. It calculates the H2 and H1 scale-height and also considers that the sun is not exactly on the galactic plane. It then calculates
the H1 and H2 density using

$$0.7 \times e^{\frac{-r}{7.0}-(\frac{1.9}{r})^2}$$

and

$$[58 \times e^{\frac{-r}{1.2}-(\frac{3.5}{r})^2}] + 240 \times e^{-(\frac{r^2}{0.095})}$$

where the last term is for the galactic center. It calculates the gas density along the line of sight, considering HI and H2 densities and their respective scale heights. The

function returns av and ebv. Av is the total extinction in the visual band caused by ISM. Ebv refers to the color excess, which represents the difference between blue and the visible band. It quantifies the reddening effect caused by the interstellar dust.

The simulator then uses the ebv values to calculate the Mg2 column density using Frisch & Slavin 2003, who explained that the fraction of Mg in the ISM that is singly ionized is 0.825, and the ISM abundance of Mg is-5.33

To calculate the column density of Mg ions, we use the formula

$$\log_{10}(nh \times fractionMg2 \times 10)^{Mg\_abn}$$

where nh represents the column density of Mg. Similarly, we calculate the column density for Fe and MgI+ ions and then use these values to call the cute_ism_abs_all function to calculate the flux.

- The cute_ism_abs_all function calculates the total ISM by multiplying the ISM of the 1st ionization state of Mg2+ ion with the 2nd ionization state of Mg2+ ion, ionization of Mg1+ ion, and Fe2+ ion. It then calculates the absorbed flux by multiplying with normalized and continuum flux and returns the absorbed flux.
    - To calculate the ISM of Mg ions, we call the Voigt function, which takes into account the Doppler parameter, Doppler width (converted into meters), and damping parameter a. It separates wings and core and further uses the formula

$$tau = 0.014971475 \times (10^{absorber[\mathrm{N}]}) \times line[\mathrm{F}] \times {}^{vo}/_{vd}$$

$$Voigt\ profile = e^{tau}$$

      The constant 0.014971475 ensures that all the units and scaling factors are correctly applied. The term (10.0 ** absorber["N"]) converts the logarithmic column density to a linear scale, giving the actual number density of absorbing atoms. The term line["F"] provides the probability of absorption for the specific spectral line, and dividing by vd normalizes it. The exponential of tau gives us the Voigt profile.
- The unred function is designed to correct the effects of interstellar dust based on the wavelength-dependent extinction curve. Specific parameters for LMC2 & AVGLMC (specified regions with different ISM characteristics) are defined using the Fitzpatrick extinction curve. This includes
    - x0 represents the central wavelength of the 2175 Å bump, which is a prominent feature in the UV extinction curve.. This bump is caused by the absorption of UV light by certain types of carbonaceous dust grains.
    - γ\gamma represents the width of the 2175 Å bump. A value indicates the range over which the bump extends in the UV spectrum.
    - c3 : This parameter measures the strength of the 2175 Å bump. A higher value of c3 indicates a stronger bump, which means that the dust grains responsible for the bump are more abundant or more efficient at absorbing UV light.
    - c4 : This parameter represents the curvature of the extinction curve in the far-UV (shorter wavelengths). The far-UV curvature accounts for the additional rise in extinction at shorter UV wavelengths.

- c2: This parameter represents the slope of the linear component of the UV extinction curve.

We construct the extinction curve for the optical and infrared region and then apply spline interpolation to smooth the curve across the entire wavelength. The extinction values for optical wavelengths are computed using polynomial evaluation, and by concatenating the infrared and optical wavelengths, we obtain the extinction curve. Finally, we multiply it with the E(B-V) value to consider color excess and return the dereddened flux.

- The Gaussbroad function smooths spectra by convolving them with a Gaussian. This is essential for noise reduction, signal enhancement, improved signal-to-noise ratio, and spectral broadening. Applying Gaussian smooths the spectra to mimic natural broadening effects and match observed data with theoretical models. The function uses properties of the Gaussian kernel. Firstly, it ensures that if the input value is too large relative to the wavelength range, it returns a flat spectrum. When the half-width at half-maximum (HWHM) is extremely large, the Gaussian kernel becomes very broad, averaging out over a large portion of data and suppressing fine details and sharp features. To avoid this, a value is assigned to the HWHM. The number of points is defined to be odd because the Gaussian kernel is symmetric about a point. The kernel's wavelength domain consists of a symmetric array of wavelengths centred around zero, and the abscissa values (xg) are used to define the Gaussian function in a convenient, normalized form relative to the specified HWHM. The Gaussian kernel is created with a specified HWHM and normalized such that its sum is 1. This normalization ensures that the convolution does not change the overall intensity of the spectrum, only smoothing it.

Extra padding is created to ensure sufficient padding on each end of the spectrum. This padding consists of three arrays combined into a single array and returns the broadened spectrum. This module also adds photon noise to the stellar spectra, where the magnitude of the noise is the square root of the number of photons per pixel, and applies a non-linearity correction to each. Additionally, it implements Mg and Fe ISM absorption at the positions of the MgI (2852.127 Å), Mg II (2795.528 Å and 2802.705 Å), and Fe II (2599.395 Å) resonance lines in the simulator. It calculates the number of observations in transit (transit duration/observed time) and transit depth for "n" transits.

RESULT

WASP- 189b

Wavelength Region [A]	SNR	Uncertainty in Transit Depth [ppm]	
		1 transit	15 transits
10cm			
MgII Band [2792.81-2804.72]	378.0355	678.7725	175.2583
MgI Band [2849.97-2853.54]	358.7413	715.2791	184.6843
FeII Band [2582.81-2586.78]	341.735	750.8746	193.875
20cm			
MgII Band [2792.81-2804.72]	765.6808	335.1268	86.5294
MgI Band [2849.97-2853.54]	720.6543	356.0655	91.9357
FeII Band [2582.81-2586.78]	687.1594	373.4216	96.417
30cm			
MgII Band [2792.81-2804.72]	1151.2513	222.888	57.5494
MgI Band [2849.97-2853.54]	1081.8694	237.1822	61.2402
FeII Band [2582.81-2586.78]	1031.7738	248.698	64.2136
40cm			
MgII Band [2792.81-2804.72]	1536.282	167.0267	43.1261
MgI Band [2849.97-2853.54]	1442.9077	177.8354	45.9169
FeII Band [2582.81-2586.78]	1376.1822	186.458	48.1432
50cm			
MgII Band [2792.81-2804.72]	1921.0945	163.5889	42.2385
MgI Band [2849.97-2853.54]	1803.8749	174.2192	44.9832
FeII Band [2582.81-2586.78]	1720.5079	182.661	47.1629

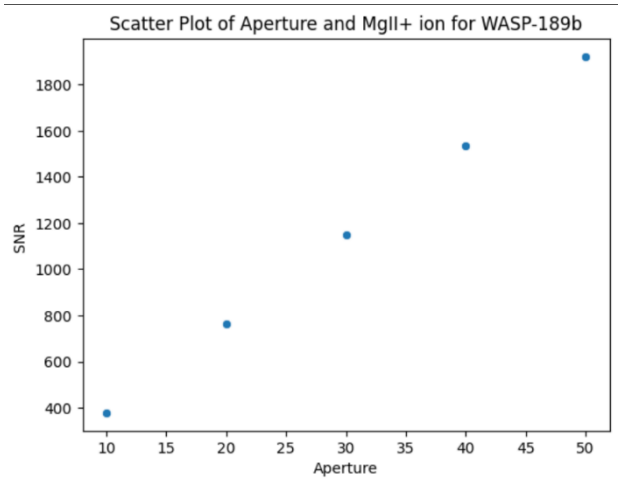

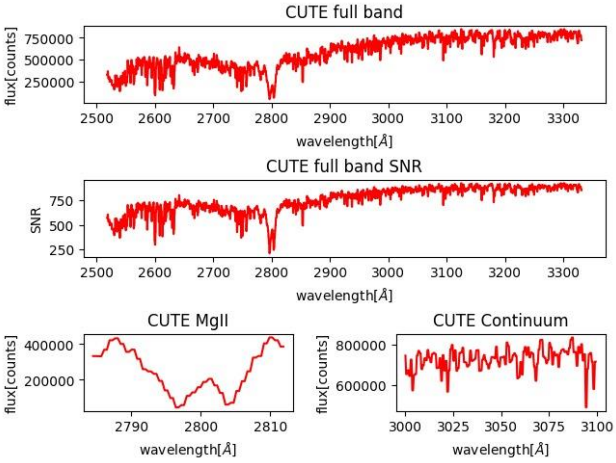

WASP-12b

Wavelength Region [A]	SNR	Uncertainty in Transit Depth [ppm]	
		1 transit	15 transits
10cm			
MgII Band [2792.81-2804.72]	17.0437	15055.3806	3887.2826
MgI Band [2849.97-2853.54]	25.3396	10126.4557	2614.6396
FeII Band [2582.81-2586.78]	25.1782	10191.3531	2631.3
20cm			
MgII Band [2792.81-2804.72]	53.291	4815.0712	1243.246
MgI Band [2849.97-2853.54]	65.4613	3919.8736	1012.107
FeII Band [2582.81-2586.78]	65.7523	3902.5249	1007.6276
30cm			
MgII Band [2792.81-2804.72]	93.3941	2747.4988	709.4011
MgI Band [2849.97-2853.54]	104.8989	2446.1668	631.5975
FeII Band [2582.81-2586.78]	105.7741	2425.9259	626.37
40cm			
MgII Band [2792.81-2804.72]	133.3343	1924.4874	496.9005
MgI Band [2849.97-2853.54]	143.4568	1788.6931	461.8386
FeII Band [2582.81-2586.78]	144.8906	1770.9917	457.2681
50cm			
MgII Band [2792.81-2804.72]	172.6225	1486.4816	383.8079
MgI Band [2849.97-2853.54]	181.5195	1413.6232	364.9959
FeII Band [2582.81-2586.78]	183.4839	1398.4883	361.0881

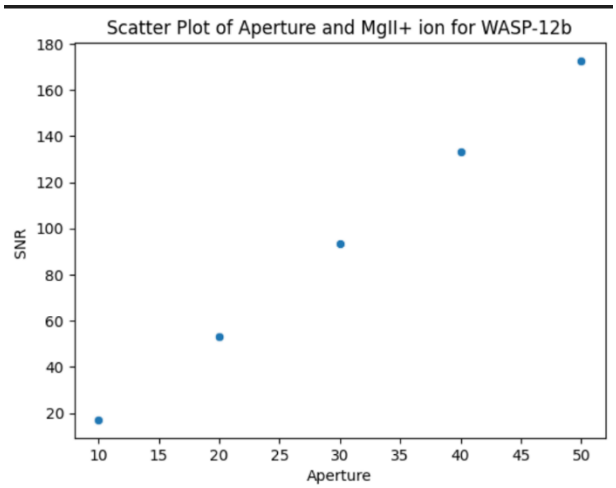

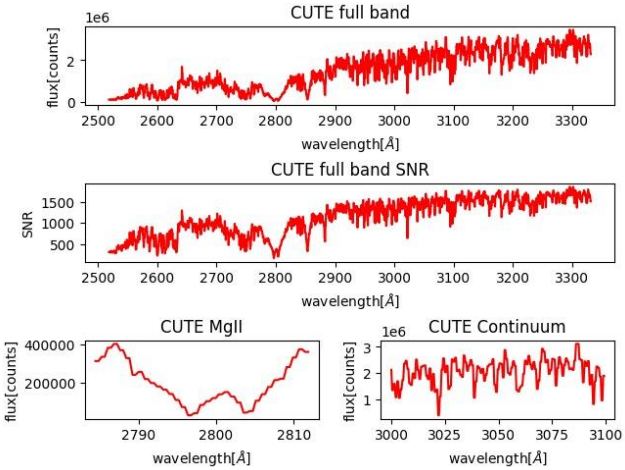

WASP-76b

Wavelength Region [A]	SNR	Uncertainty in Transit Depth [ppm]	
		1 transit	15 transit
10cm			
MgII Band [2792.81-2804.72]	10.942	28721.3817	7415.8289
MgI Band [2849.97-2853.54]	14.4887	21690.7468	5600.5268
FeII Band [2582.81-2586.78]	16.0855	19537.483	5044.5564
20cm			
MgII Band [2792.81-2804.72]	36.646	8575.8145	2214.2658
MgI Band [2849.97-2853.54]	41.9263	7495.7708	1935.3997
FeII Band [2582.81-2586.78]	46.0149	6829.7353	1763.430
30cm			
MgII Band [2792.81-2804.72]	67.3618	4665.3963	1204.6002
MgI Band [2849.97-2853.54]	70.422	4462.6662	1152.2555
FeII Band [2582.81-2586.78]	76.866	4088.5417	1055.6569
40cm			
MgII Band [2792.81-2804.72]	98.9202	3177.0026	820.2985
MgI Band [2849.97-2853.54]	98.3683	3194.8276	824.9009
FeII Band [2582.81-2586.78]	107.088	2934.686	757.7327
50cm			
MgII Band [2792.81-2804.72]	130.237	2413.059	623.0492
MgI Band [2849.97-2853.54]	125.8334	2497.5068	644.8535
FeII Band [2582.81-2586.78]	136.7973	2297.3389	593.1703

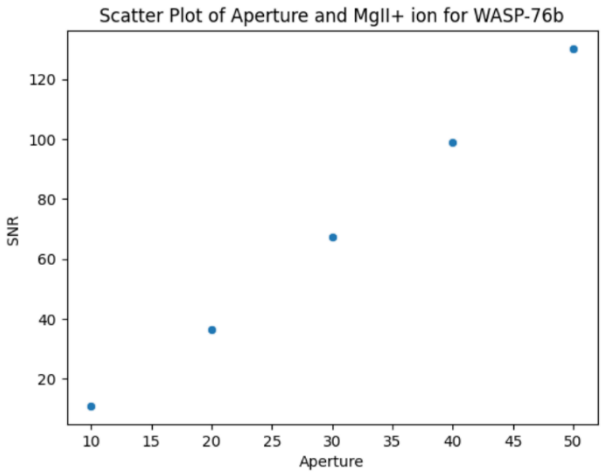

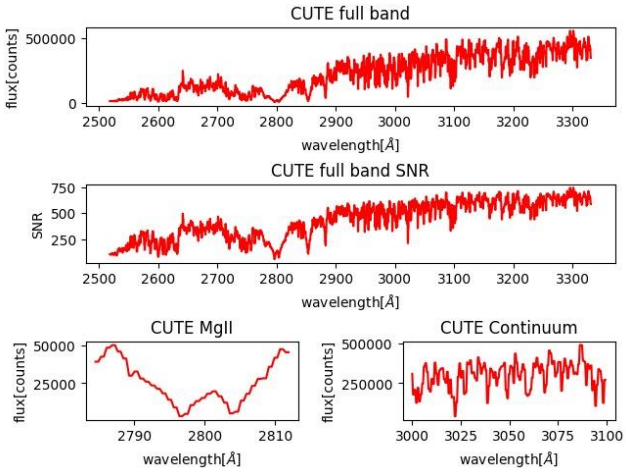

Tau Ceti e

Wavelength Region [A]	SNR	Uncertainty in Transit Depth [ppm]	
		1 transit	15 transits
10cm			
MgII Band [2792.81-2804.72]	1627.7013	20.352	5.2549
MgI Band [2849.97-2853.54]	1473.2342	22.4859	5.8058
FeII Band [2582.81-2586.78]	1614.063	20.5239	5.2993
20cm			
MgII Band [2792.81-2804.72]	3257.7382	10.1687	2.6255
MgI Band [2849.97-2853.54]	2947.2752	11.2399	2.9021
FeII Band [2582.81-2586.78]	3228.9337	10.2594	2.649
30cm			
MgII Band [2792.81-2804.72]	4887.2569	6.7782	1.7501
MgI Band [2849.97-2853.54]	4421.1369	7.4929	1.9346
FeII Band [2582.81-2586.78]	4843.6249	6.8393	1.7659
40cm			
MgII Band [2792.81-2804.72]	6516.6457	5.0834	1.3125
MgI Band [2849.97-2853.54]	5894.9539	5.6195	1.451
FeII Band [2582.81-2586.78]	6458.2713	5.1294	1.3244
50cm			
MgII Band [2792.81-2804.72]	8145.9826	4.0667	1.05
MgI Band [2849.97-2853.54]	7368.7529	4.4956	1.1608
FeII Band [2582.81-2586.78]	8072.8997	4.1035	1.0595

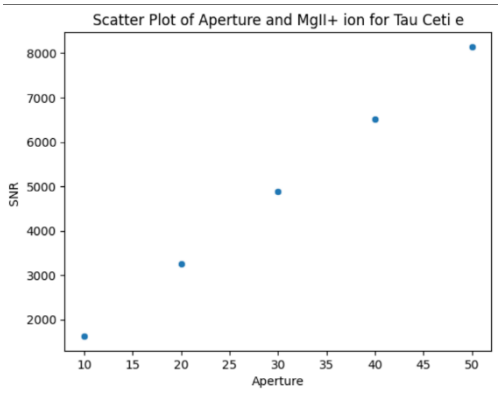

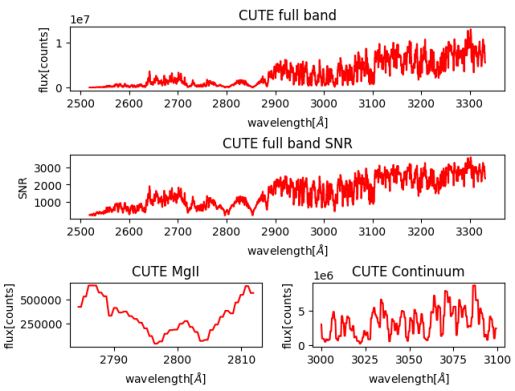

OBSERVATION

We have analyzed data from several planets observed by the CUTE satellite and Tau Ceti e, which has a star similar to the sun.

- We found that a higher signal-to-noise ratio (SNR) increases the likelihood of detecting elements in a planet's atmosphere. The uncertainty in SNR decreases as the number of transits increases.

- In addition, we discovered that the SNR of a planet increases with the aperture size of the instrument, which affects the total effective area of the instrument capable of detecting incoming rays.

- Furthermore, we observed that the SNR increases as the parallax increases due to the inverse relationship between the distance of the star and the parallax. The incoming signal would increase with parallax, while noise would remain constant, as it depends on the instrument. Therefore, we observe a linear increase in the graph.

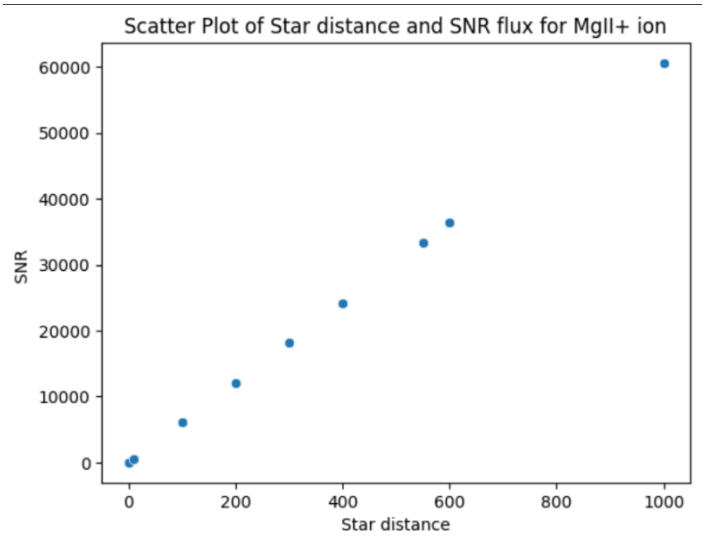

REFERENCES

- https://arxiv.org/pdf/1903.03314
- https://www.researchgate.net/publication/369855727_The_Colorado_Ultraviolet_Transit_Experiment_CUTE_signal_to_noise_calculator
- https://exoplanet.eu/home

Prashant Pathak

Space, Planetary & Astronomical Sciences & Engineering (SPASE)

MENTOR SIGNATURE